Journal of Food Engineering 120 (2014) 268–276

Contents lists available at ScienceDirect

Journal of Food Engineering

journal homepage: www.elsevier.com/locate/jfoodeng

Radio frequency disinfestation treatments for dried fruit: Model development and validation

Bandar Alfaifi [a,b], Juming Tang [a,*], Yang Jiao [a], Shaojin Wang [c], Barbara Rasco [d], Shunshan Jiao [a], Shyam Sablani [a]

[a] Department of Biological Systems Engineering, Washington State University, Pullman, WA 99164-6120, USA
[b] Agricultural Engineering Department, King Saud University, P.O. Box 2460, Riyadh 11451, Saudi Arabia
[c] College of Mechanical and Electronic Engineering, Northwest A&F University, Yangling, Shaanxi 712100, China
[d] School of Food Science, Washington State University, Pullman, WA 99164-6376, USA

ARTICLE INFO

Article history:
Received 14 March 2013
Received in revised form 18 June 2013
Accepted 15 July 2013
Available online 23 July 2013

Keywords:
RF heating
Heating uniformity
Computer simulation
Dielectric properties
Dried fruits

ABSTRACT

Non-uniform heating is one of the most important challenges during the development of radio frequency (RF) heat treatments for pest control and other applications. A computer simulation model using finite element-based commercial software, COMSOL, was developed to investigate the heating uniformity of raisins packed in a rectangular plastic container ($25.5 \times 15.0 \times 10.0\ cm^3$) and treated in a 6 kW, 27.12 MHz RF system. The developed model was then experimentally validated. Simulated and experimental temperature distributions in raisins after RF heating were compared in three different horizontal layers (top, middle, and bottom) within the container. Simulated and experimental average and standard deviation of the temperature values were highest in the middle layer, followed by the top and bottom layers. A sensitivity study indicated that the heating uniformity of the samples was most affected by the density of the raisins followed by the top electrode voltage, the dielectric properties, the thermal conductivity and the heat transfer coefficient. Corners and edges were heated more than the centers in each layer of the RF treated raisins. The model developed here can be used for future investigations to improve the heating uniformity for insect disinfection of dried fruit and other similar applications.

1. Introduction

Insect infestation is one of the most important sanitary or quarantine considerations limiting domestic and international trade of dried fruits including raisins, dates, apricots, figs, and prunes. Postharvest control of insects that attack dried fruits such as: Indianmeal moth (*Plodia interpunctella*), navel orangeworm (*Amyelois transitella*), raisin moth (*Cadra figulilella*), fig moth (*Ephestia cautella*), driedfruit beetle (*Carpophilus hemipterus*), and sawtoothed grain beetle (*Oryzaephilus surinamensis*) is essential if quarantine regulations required in many countries (Johnson et al., 2009) are to be met. On the other hand, total postharvest product losses from insect infestation are conservatively estimated to be between 10% and 40% worldwide through direct damage; contamination with fecal matter, webbing and insect parts (Pimentel and Raman, 2002). Insect infestation promotes increased mold growth, toxin production, and product degradation. Traditionally, chemical fumigation has been the most widely used treatment for insect control due to its efficacy and relatively low cost (Barreveld, 1993). However, environmental and public health concerns about the hazards of chemical fumigation have increased the demand for non-chemical pest control methods for dried fruits.

The interest in non-chemical methods for insect disinfestations in agricultural commodities has grown in recent years due to increased food and environmental safety requirements. One alternative to chemical fumigation is radio frequency (RF) treatment, which has been shown to be lethal to insects at low intensity (Wang et al., 2007b). RF dielectric heating employs electromagnetic waves of 13.56, 27.12, and 40.68 MHz for industrial applications (Metaxas, 1996). However, major challenges with adopting RF heating in the food industry are non-uniform heating and runaway heating, which cause overheating in corners, edges, and center parts, especially in foods of intermediate and high water content (Fu, 2004). Temperature variations among and within processed agricultural commodities reduce the efficiency of a treatment and may cause severe thermal damage to its quality and adversely affect product safety. During RF processing, several interacting factors influence heating uniformity (Wang et al., 2005). These factors include the design of RF heating systems (e.g. the electrode shape and power output), packaging geometries, dielectric, thermal and physical properties of the treated materials,

* Corresponding author. Address: 213 LJ Smith Hall, Pullman, WA 99164-6120, USA. Tel.: +1 509 335 2140; fax: +1 509 335 2722.
E-mail address: jtang@wsu.edu (J. Tang).

0260-8774/$ - see front matter © 2013 Elsevier Ltd. All rights reserved.
http://dx.doi.org/10.1016/j.jfoodeng.2013.07.015

position of the treated materials within the RF units, and the surrounding media (Fu, 2004).

The trial and error procedure often practiced to adjust these parameters to improve the heating uniformity is ineffective and costly. Mathematical modeling and computer simulation serve as valuable tools for shedding light on the complex mechanisms underlying the heating uniformity of food products subjected to RF treatments without the necessity of extensive time consuming experiments. The first attempt to model RF systems was reported in the 1990s (Neophytou and Metaxas, 1996, 1997, 1998, 1999). These efforts attempted to model the electrical field for industrial-scale RF heating systems and compared solutions from both electrostatic and wave equations. Yang et al. (2003) investigated temperature distributions for alfalfa and radish seeds placed inside rectangular polystyrene boxes after RF heating using commercial software TLM-FOOD HEATING. The developed model was then validated with experimental data. Chan et al. (2004) developed an effective model to simulate an actual RF heating system using a finite elements method to solve wave equations. The simulated and experimental data for different sized loads and positions of a 1% solution of carboxymethyl cellulose showed good agreement. Marra et al. (2007) analyzed the temperature profiles of cylindrical meat batters treated with a 50 Ω, 27.12 MHz RF system at different output power levels using commercially available finite element-based software, FEMLAB. The model was then validated by comparing simulated and measured temperature profiles. The authors reported uneven temperature distributions within the sample; the higher the applied power, the more uneven the temperature distribution. Heating non-uniformity in fresh fruits subjected to a 12 kW, 27.12 MHz RF system has been investigated mathematically using FEMLAB (Birla et al., 2008). Factors such as dielectric properties, shape, surrounding media, and position of fruit were found to affect the heating uniformity of fresh fruits. Tiwari et al. (2011a) developed and validated a computer simulation model for a 12 kW, 27.12 MHz RF system using COMSOL to compare the simulated temperature profiles of wheat flour with transient experimental temperature profiles in RF heating. The validated model was further used to predict the influence of the shape, positions, configuration of the top electrode, and other related factors on the RF power distribution in dry food materials (Tiwari et al., 2011b).

There are no reports on the computer simulation for RF heating of high sugar and intermediate moisture materials. To investigate the RF heating characteristics in these materials and select operational parameters to improve the RF heating uniformity, it is desirable to develop a computer simulation model and validated it by experiment. The objectives of this study were to investigate RF heating behavior in raisins using computer simulation, estimate dielectric properties and thermal conductivity of raisins packed in a container using published mixture equations, develop computer simulation model for a 6 kW, 27.12 MHz RF system using commercial finite element software COMSOL, and validate the computer model with experimental temperature profiles of raisins.

2. Materials and methods

2.1. Development of computer model

2.1.1. Physical model

A free-running oscillator, 6 kW, 27.12 MHz parallel plate RF heating system (COMBI 6-S, Strayfield International Limited, Wokingham, UK) was used for the RF heating experiments. Fig. 1 provides a schematic view of the RF unit used in this study. The RF system consisted of a generator and an applicator comprising a pair of parallel plate electrodes inside a large rectangular metallic enclosure. The electrodes were connected to a tank oscillatory circuit. The samples were sandwiched between the two electrodes. This configuration has been shown to achieve greater temperature uniformity in the top and bottom layers in a container (Tiwari et al., 2011b).

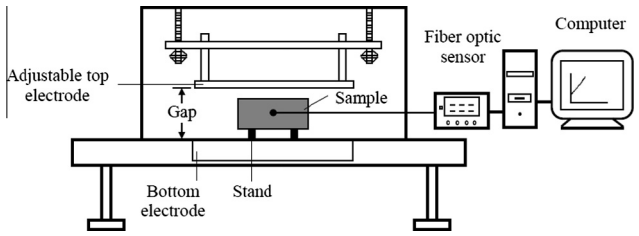

Fig. 1. Schematic view of the pilot-scale 6 kW, 27.12 MHz RF unit showing the rectangular plastic container placed in between the top and bottom electrodes (Adapted from Wang et al., 2010).

2.1.2. Governing equations

2.1.2.1. Electric current. A quasi-static approximation was used to solve Maxwell's electromagnetic field equations. Since the wavelength (11 m) in the 27.12 MHz RF system is often much larger than the electrode gap, Maxwell's equations were simplified to Laplace equations (Metaxas, 1996):

$$-\nabla \cdot ((\sigma + j2\pi f \varepsilon_0 \varepsilon')\nabla V) = 0 \quad (1)$$

where σ is the electrical conductivity of the heated material (S m^{-1}), $j = \sqrt{-1}$, f is the frequency (Hz), ε_o is the permittivity of free space (8.86×10^{-12} F m^{-1}), ε' is the dielectric constant of the material, and V is the voltage between the two electrodes (V). The electric field strength is $\vec{E} = -\nabla V$.

2.1.2.2. Heat transfer. The heat conduction was considered within the food material, convection at the material's surface, and heat generation due to RF heating. The governing heat transfer equation in the electromagnetic field is described as:

$$\rho C_P \frac{\partial T}{\partial t} = \nabla \cdot (k \nabla T) + Q \quad (2)$$

where ρ is the density (kg m^{-3}), C_p is the specific heat of the heated material (J kg^{-1} K^{-1}), T is the temperature inside the material (°C), t is the process time (s), k is thermal conductivity (W m^{-1} K^{-1}), and Q is the RF power conversion to thermal energy (W m^{-3}) within the food material for a given electric field intensity, $\vec{E}$. Q is described as (Choi and Konrad, 1991):

$$Q = 2\pi f \varepsilon_0 \varepsilon'' |\vec{E}|^2 \quad (3)$$

where $|\vec{E}|$ is the magnitude of electric field intensity (V m^{-1}).

2.1.3. Geometrical, thermal, and electrical boundary conditions

Figs. 2 and 3 show the geometrical, thermal and electrical boundary conditions of the 6 kW, 27.12 MHz RF system used in the simulation. Electrical insulation ($\nabla \cdot \vec{E} = 0$) and thermal insulation ($\nabla T = 0$) were assigned to the inlet and outlet of the system, while electrical insulation ($\nabla \cdot \vec{E} = 0$) only was assigned to the walls of the RF applicator. The bottom electrode was set as ground ($V = 0$ V). The top exposed surface of the sample was assigned with convective heat transfer ($h = 20$ W m^{-2} K^{-1}) for free convection of ambient air. The raisin samples were equilibrated at room temperature prior to RF heating and, therefore, it was assumed that these samples were at a uniform temperature, $T_{initial}$. In all cases, the initial temperature, $T_{initial}$, was set at 23 °C. The voltage on the top electrode was assumed to be uniformly distributed because its dimensions (68.6×49.5 cm^2) were only 30% of the RF wavelength

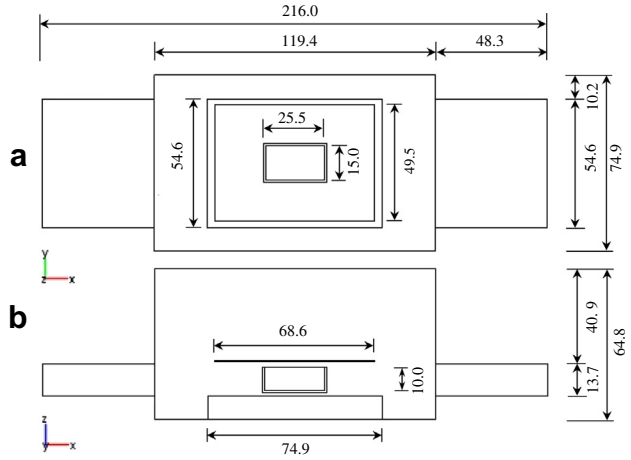

Fig. 2. Geometrical boundary conditions of (a) top view and (b) front view of a 6 kW, 27.12 MHz RF system used in simulations (dimensions are in cm).

of 27.12 MHz (11 m) (Barber, 1983). The voltage was also assumed to be constant during the RF treatment because it varies by only 7% in typical industrial-scale RF systems between standby to full load position (Metaxas, 1996).

2.1.4. Solution methodology

A finite element method was used to solve the coupled electromagnetic and heat transfer equations (Joule heating model) using commercial software, COMSOL (V4.2a, COMSOL Multiphysics, Burlington, MA, USA). The software was run on a US Micro Mini-Tower Workstation with a Core i7-2600, 3.4 GHz Quad Core Processor and 16 GB RAM operating with a Windows 7 64-bit operating system. Fig. 4 illustrates the steps taken in the simulation. An unstructured mesh consisting of a Lagrange quadratic element was generated over the entire domain of the RF cavity. Finer mesh was created near the sharp edges and corners of the sample and the container to increase the accuracy of the solution. Mesh convergence study was performed to verify that the results were independent on the mesh size. This verification was accomplished by running the same simulation with several different types of meshes to determine what, if any, effect it would have on the results. Five meshes were created; these meshes are designated by COMSOL to be Normal, Fine, Finer, Extra fine, and Extremely fine. Table 4 shows properties of these meshes. Mesh size was considered when the difference in the resulted temperatures between successive calculations was less than 0.1%. The direct linear system solver UMFPACK was used with a relative tolerance and an absolute tolerance of 0.01 and 0.001, respectively. Initial and maximum time steps were set as 0.001 and 1 s.

2.1.5. Model parameters

Information on the dielectric, thermal, and physical properties of the sample and the surrounding medium are essential in modeling the RF heating process. Tables 1 and 2 summarize these values. The density was assumed to be temperature independent, whereas the thermal conductivity, specific heat, and dielectric properties of the materials were assumed to be temperature dependent over the range of treatment temperatures (20–60 °C) suitable for postharvest pest control.

Foods such as fruits, vegetables, and foodstuffs in bulk may contain certain amounts of air, which impedes the flow of heat throughout the heated material during the heating process. It is impractical to measure dielectric and thermal properties for such materials with different densities. Therefore, six well-known mixture equations were used to estimate the effective dielectric and thermal conductivity of the air-particle mixture using Matlab 2010 (Mathworks Inc., Natick, MA). The dielectric properties of raisin paste (0% air) at the particle density, 1422 kg m^{-3}, obtained from Alfaifi et al. (2013) and the thermal properties (thermal conductivity and specific heat) measured in this study using the dual needle probe method (KD2 Pro, Decagon Devices, Pullman, USA) within the temperature range from 20 to 60 °C were used in the mixture equations. These data are listed in Table 1. Dielectric mixture equations have been widely used to estimate the dielectric properties of a bulk mass from the properties of an air-particle mixture made up of air (voids) and particles of the solid (Nelson, 1991, 1992). These equations relate the dielectric properties and the bulk density. For the dielectric properties, the following equations were used:

Complex Refractive Index mixture equation (CRIME) (Kraszewski, 1977):

$$\varepsilon^{\frac{1}{2}} = v_1(\varepsilon_1)^{\frac{1}{2}} + v_2(\varepsilon_2)^{\frac{1}{2}} \quad (4)$$

Landau and Lifshitz, Looyenga equation (LLLE) (Landau and Lifshitz, 1960; Looyenga, 1965):

$$\varepsilon^{\frac{1}{3}} = v_1(\varepsilon_1)^{\frac{1}{3}} + v_2(\varepsilon_2)^{\frac{1}{3}} \quad (5)$$

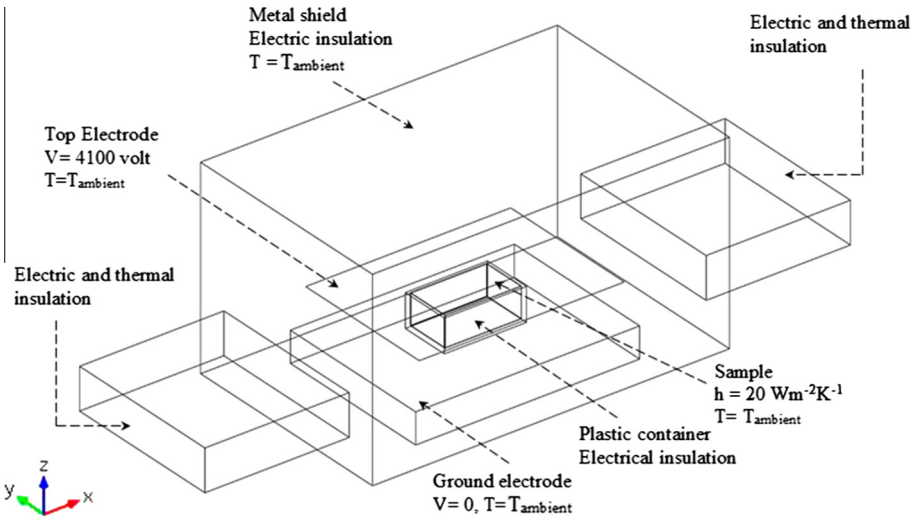

Fig. 3. Thermal and electrical boundary conditions of the 6 kW, 27.12 MHz RF system used in simulation.

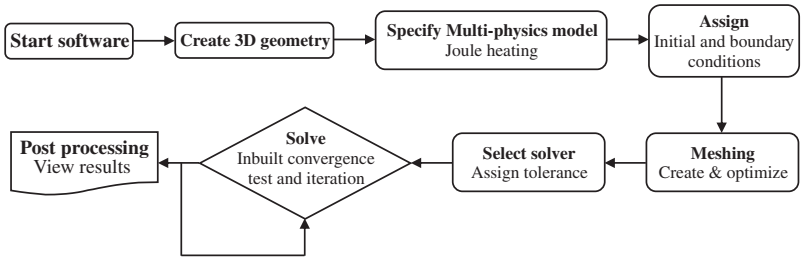

Fig. 4. Flow chart of modeling steps using COMSOL Multiphysics V4.2a.

Table 1
Dielectric and thermal properties (Mean ± standard deviation) of raisins at 27 MHz, five temperatures, and a particle density of 1422 kg m^{-3}.

Temp. (T, °C)	Dielectric constant (ε')*	Loss factor (ε'')*	Thermal conductivity (k, W m^{-1} K^{-1})	Specific heat (C_p, J kg^{-1} K^{-1})
20	21.9 ± 0.1	8.1 ± 0.1	0.315 ± 0.002	2048.4 ± 25.4
30	24.8 ± 0.4	8.9 ± 0.1	0.337 ± 0.005	2150.8 ± 15.2
40	28.0 ± 0.4	9.8 ± 0.2	0.345 ± 0.003	2279.4 ± 28.6
50	31.2 ± 0.3	10.6 ± 0.1	0.368 ± 0.005	2360.5 ± 12.8
60	33.8 ± 0.3	11.4 ± 0.1	0.379 ± 0.004	2486.4 ± 19.5

* From Alfaifi et al. (2013).

Table 2
Electrical and thermo-physical properties of materials used in computer simulation.

Materials properties	Aluminum*	Polypropylene*	Air*
Thermal conductivity (k, W m^{-1} K^{-1})	160	0.2	0.025
Density (ρ, kg m^{-3})	2700	900	1.2
Specific heat (C_p, J kg^{-1} K^{-1})	900	1800	1200
Dielectric constant (ε')	1	2.0**	1
Loss factor (ε'')	0	0.0023**	0

Source.
* COMSOL material library, V4.2a (2012).
** von Hippel (1995).

Bottcher equation (BE) (Bottcher, 1945):

$$\frac{\varepsilon - \varepsilon_1}{3\varepsilon} = v_2 \frac{\varepsilon_2 - \varepsilon_1}{\varepsilon_2 + 2\varepsilon} \tag{6}$$

where ε is the complex permittivity of the mixture, ε_1 is the permittivity of the medium (air), ε_2 is the permittivity of solid (raisins), v_1 is the volume fraction of the medium (air), and v_2 is the volume fractions of solid (raisin porosity $v_2 = e = 0.45$), where $v_1 + v_2 = 1$. These equations have been used successfully to predict the dielectric properties of various granular materials (Nelson, 1991, 1992). Both granular and porous foods are two-media systems composed of air and solids; therefore, models developed for granular foods can also be used for porous foods such as bread (Liu et al., 2009) with an error of ±10% and biscuit dough (Kim et al., 1998) with an error range of ±1.98% to 2.85%.

For thermal conductivity, the following mixture equations were used:

Parallel model:

$$k_e = \sum_i k_i v_i \tag{7}$$

Kopelman model (Kopelman, 1966):

$$k_e = k_c \left(\frac{1 - v_2^{2/3}(1 - (k_d/k_c))}{1 - v_2^{2/3}(1 - (k_d/k_c))(1 - v_2^{2/3})} \right) \tag{8}$$

Maxwell–Eucken model (Eucken, 1940):

$$k_e = k_c \left(\frac{2k_c + k_d - 2v_2(k_d - k_c)}{2k_c + k_d + 2v_2(k_d - k_c)} \right) \tag{9}$$

where k_e is the effective thermal conductivity for the bulk mass, W m^{-1} K^{-1}, k_c is the thermal conductivity of solid, W m^{-1} K^{-1}, k_d is the thermal conductivity of air, W m^{-1} K^{-1}, and v_2 is the volume fraction of the air.

During the operation of an RF system, it is difficult to accurately measure the voltage of the top electrode (Marshall and Metaxas, 1998). Therefore, preliminary simulations were run by considering different values for the voltage of the top electrode and the resulting temperature distribution was compared with the experimental temperature distribution during treatment. Based on the preliminary simulated and experimental temperature distribution, the voltage of the top electrode was set as 4100 V for all simulation runs. The same method has been used to estimate the top electrode voltage of similar RF systems (Marshall and Metaxas, 1998; Birla et al., 2008; Tiwari et al., 2011a). Information of electrical and thermo-physical properties of materials used in computer simulation is listed in Table 2.

Acceptable mortality levels (~99.83%) of the navel orangeworm (*A. transitella*), which is one of the most resistant insects in dried fruits (Wang et al., 2007c), for industrial use to process large volumes requires temperatures 52 °C and 55 °C at an exposure time 6 min and 1 min, respectively, and a heating rate 5–10 °C min^{-1} (Wang et al., 2002). This heating rate range can be achieved by using an electrode gap of 13, 13.6, or 14.2 cm (Fig. 6) Therefore, 13.6 cm gap was used in further simulations and experiments. The minimum temperature in this study to disinfest insects was 52 °C based on the resulted non-heating uniformity, the preliminary results, and especially the overheating around the edges and corners.

The relative sensitivity with respect to model inputs was evaluated using the uniformity index (UI) of the treated samples in simulation. This index is a useful tool to evaluate the heating uniformity when using a fixed configuration and a specific RF unit. It is defined as:

$$UI = \frac{\frac{1}{V_{vol}} \int_{V_{vol}} \sqrt{(T - T_{av})^2} dV_{vol}}{T_{av} - T_{\text{initial}}} \tag{10}$$

where V_{vol} is the material volume (m^3), and T and T_{av} are local and average temperatures (°C) inside the dielectric material over the volume (V_{vol}, m^3). The smaller the UI value, the better the RF heating

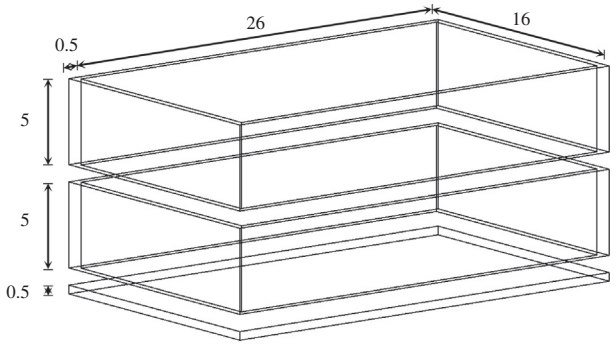

Fig. 5. Rectangular plastic container split into three parts for temperature profile measurements (all dimensions are in cm).

uniformity. The minimum value of UI is zero, which indicates uniform temperature in dielectric material.

2.2. Model validation

2.2.1. Experimental procedure

To validate the computer simulation model, the 6 kW, 27 MHz pilot-scale RF system (Strayfield Fastran with E-200, Strayfield International Limited, Wokingham, UK) described above was used to heat Thompson seedless raisins (*V. vinifera*) (Caruthers Raisin Packing, Caruthers, CA). Raisins were stored under refrigeration (5 °C) until tests. The initial water content of raisins was approximately 15% (w.b.). A rectangular container (25.5 L × 15.0 W × 10.0 H cm^3) made of polypropylene divided into two parts and separated by a very thin plastic layer of mesh (thickness 2 mm with mesh opening of 1.3 mm) was used to facilitate temperature mapping in the middle layer. A removable bottom base with thickness 0.5 cm was used to facilitate temperature mapping in the bottom layer. The rectangular container is shown in Fig. 5. About 3 kg of raisins (bulk density of 784 kg/m^3) were placed into the containers and positioned in the center and middle plane between the two electrodes. Prior to the RF treatment, the samples were equilibrated at room temperature. The temperature in the center of the samples was measured using pre-calibrated FISO optic sensors (UMI, FISO Technologies Inc., Saint-Foy, Quebec, Canada) during RF heating. Before and after the RF treatment, the temperature distribution of the upper surfaces of each sample in the three layers: top, middle, and bottom, in the container were evaluated using an infrared camera (Thermal CAM™ SC-3000, N. Billerica, MA, USA) having an accuracy of ±2 °C. Details on the measurement procedure and the precision of this camera can be found in Wang et al. (2007a). The total measurement time for the three layers was about 30 s. ThermaCAM Researcher 2001 software (FLIR Systems AB, N. Billerica, MA, USA) was used to collect and analyze the surface temperature data points for each layer. Mean values and standard deviations of the three horizontal layer, top, middle, and bottom temperatures were calculated from five replicates.

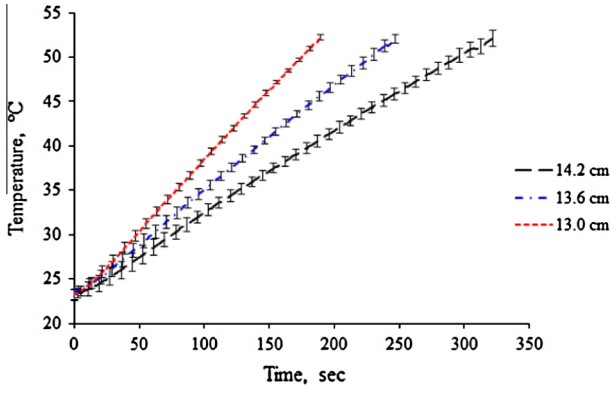

Fig. 6. Temperature–time histories of the RF heated raisins (to a center temperature of 52 °C) in the center of the 10 cm thick container as a function of the electrode gap.

3. Results and discussion

3.1. Dielectric and thermal properties of samples

The influence of the temperature on the dielectric and thermal properties of raisins at 27 MHz are given in Table 1. The dielectric constant and loss factor of raisins increased when temperature increased from 20 to 60 °C. More information about the dielectric properties of raisins can be found elsewhere in Alfaifi et al. (2013). Likewise, both thermal conductivity and specific heat of the samples increased from 0.32 to 0.38 W m^{-1} K^{-1} and 2048 to 2486 J kg^{-1} K^{-1}, respectively, in a linear fashion, although the change in the thermal conductivity was slightly less than that of the specific heat over the temperature range used in this study.

The dielectric properties and the thermal conductivity of raisins at a bulk density of 784 kg m^{-3} calculated from the mixture equations are presented in Table 3. As expected, due to the presence of air, the dielectric properties and the thermal conductivity of the bulk raisin samples were reduced compared to these properties of the raisin paste (0% air). The values of the dielectric properties calculated from the LLLE model were slightly smaller compared with those calculated from the CRIME and BE models. The values of the thermal conductivity calculated from the Maxwell–Eucken model were smaller compared with those calculated using the Kopelman and parallel models. The differences between the values obtained from these models ranges from 16–20%, 29–32%, and 11–15% for the dielectric constant, loss factor, and thermal conductivity, respectively, at a temperature range 20–60 °C.

3.2. Simulated temperature profiles for raisin samples

A mesh convergence study was conducted considering different number of elements used in the model (Table 4). Temperature distribution was modeled for RF heating simulation for 4 min at a fixed gap of 13.6 cm and initial temperature of 23 °C. When the difference in maximum and minimum temperature values of the sample between two sequential sets of meshes was less than 0.1%, temperature distribution was considered to be independent of mesh size. Extra fine and extremely fine mesh sets provided similar temperature distributions. The final mesh system consisted of 404,506 domain elements (tetrahedral), 41,648 boundary elements (triangular), and 2135 edge elements (linear), were used in subsequent simulation runs.

Table 5 compares the temperature profiles of RF heated raisin samples treated for 4 min at a fixed gap of 13.6 cm in three horizontal layers, top, middle, and bottom using different combinations of the dielectric and thermal conductivity properties estimated from different mixture equations. Little difference was shown in temperatures over the range of properties selected for the model. The LLLE and Kopelman models were used in further simulations because the smallest variation was shown.

Fig. 7a–c shows the simulated temperature profiles of treated raisins in three horizontal (0, 5, and 10 cm) and three vertical (0, 12.8, and 25.5 cm) layers and whole sample after 4 min RF heating at a fixed gap of 13.6 cm and an initial temperature of 23 °C. The simulation was conducted using the dielectric properties and thermal conductivity values estimated from LLLE and Kopelman

Table 3
Estimated dielectric properties and thermal conductivity of raisins as a function of temperature using three different mixture equations for bulk density of 784 kg m^{-3}.

Temp. (°C)	Dielectric properties						Thermal conductivity		
	CRIME*		BE		LLLE		Parallel	Kopelman	Maxwell--Eucken
	ε'	ε''	ε'	ε''	ε'	ε''	k (W m^{-1} K^{-1})		
20	9.2	2.9	8.6	2.7	7.9	2.2	0.181	0.164	0.157
30	10.2	3.1	9.6	3.0	8.7	2.4	0.191	0.174	0.167
40	11.3	3.4	10.6	3.2	9.6	2.6	0.200	0.184	0.177
50	12.4	3.7	11.7	3.5	10.4	2.8	0.210	0.193	0.187
60	13.3	3.9	12.5	3.8	11.1	3.0	0.218	0.202	0.196

BE: Bottcher equation.
LLLE: Landau and Lifshitz, Looyenga equation.
* CRIME: Complex Refractive Index mixture equation.

Table 4
Simulated (LLLE x Kopelman) temperature (°C) distributions of sample for top, middle, and bottom layers after 4 min RF heating at a fixed electrode gap of 13.6 cm and initial temperature 23 °C as a function of mesh density.

Type of mesh	Tetrahedral	Triangular	Edge	Solution time (min:sec)	Top layer*			Middle layer			Bottom layer		
					Max.	Min.	Center	Max.	Min.	Center	Max.	Min.	Center
Normal	87,966	19,407	1611	05:54	67.3	40.9	41.1	77.6	45.3	52.1	62.3	39.2	40.0
Fine	131,792	21,726	1683	07:57	64.8	40.8	40.8	77.3	44.1	52.0	60.3	39.2	39.4
Finer	217,640	29,923	1852	13:38	62.8	40.9	40.9	77.1	44.1	52.0	58.7	39.4	39.3
Extra fine	404,506	41,698	2135	26:13	62.8	40.9	41.0	77.1	44.3	52.0	57.6	39.4	39.4
Extremely fine	622,181	52,238	2470	41:12	62.7	40.9	41.2	77.1	44.3	52.0	57.5	39.4	39.4

* All temperatures are in °C.

equations. In the horizontal layers, the temperatures were highest in the middle layer (45–76 °C), whereas they were lower in the top and the bottom layers (41–62 °C and 40–57 °C). In the horizontal layers, the highest temperature values were at the corners and edges of all layers except for the middle layer. It is well known that RF volumetric heating occurs throughout the whole food simultaneously. However, factors such as food shape, volume, surface area, composition, dielectric and thermal properties, surrounding media, and the design of the RF system could cause the electromagnetic field to unevenly distribute. The low temperature values of the outer surfaces of the sample might be attributed to the evaporative cooling between the outer surfaces of the sample and the surrounding area. Overheating was observed at the edges and corners of the top (51 and 62 °C), middle (65 and 76 °C), and bottom (48 and 57 °C) layers (Fig. 8a). This behavior could be attributed to the refraction and reflection of the electrical field at interfaces. When the radiation wavelength is larger than the dimensions of the heated object, as is the case with RF radiation used in this study, field bending causes the electrical field to be concentrated at some locations. The merging of two or more waves at the edges and corners result in a higher volumetric power density, hence, overheating occurs in these areas more than on the flat surfaces (Yang and Pearce, 1989). This behavior has been observed for walnuts (Wang et al., 2007a), heterogeneous foods (Wang, 2007), and wheat flour (Tiwari et al., 2011a) subjected to RF treatment. More uniform temperature distribution were obtained in the flat area of the top (41–45 °C) and the bottom (40–44 °C) layers with less uniformity observed in the middle layers (52–59 °C). The less uniform temperature values in the flat area of the middle layer could be due to the result of the field bending at the sides of the sample and concentrating in the middle, as well as heat transfer by conduction inside the sample during the RF heating.

3.3. Model validation

Fig. 8b shows the experimental temperature distribution of the sample of raisins in three horizontal layers: top, middle, and bottom after 4 min RF heating at a fixed gap of 13.6 cm and an initial temperature 23 °C. In general, the experimental results showed good agreements with the simulated data. When comparing the

Table 5
Simulated temperature (°C) profiles of RF heated raisins sample for 4 min at a fixed gap of 13.6 cm in three horizontal layers, top, middle, and bottom, using estimated dielectric properties and thermal conductivity from six different models.

Thermal conductivity models	Layer	Dielectric properties models											
		CRIME				BE				LLLE			
		Max.	Min.	Center	Ave.	Max.	Min.	Center	Ave.	Max.	Min.	Center	Ave.
Kopelman	Top	67.1	40.7	40.9	51.4	67.5	41.4	41.6	52.1	62.8	40.9	41.0	50.2
	Middle	79.2	45.3	51.9	62.4	80.6	45.8	52.9	63.6	77.1	44.3	52.0	61.6
	Bottom	61.3	39.3	39.3	46.7	61.5	39.9	40.0	47.3	57.6	39.4	39.4	45.8
Parallel	Top	67.1	40.6	40.8	51.3	67.5	41.3	41.5	51.9	62.6	40.7	40.9	49.9
	Middle	79.4	45.1	51.9	62.5	80.8	45.6	52.9	63.6	77.0	44.0	52.0	61.4
	Bottom	61.2	39.2	39.2	46.6	61.4	39.8	39.8	47.2	57.3	39.2	39.3	45.5
Maxwell-Eucken	Top	67.1	40.5	40.7	51.2	67.5	41.3	41.5	51.9	62.7	40.6	40.9	49.9
	Middle	79.4	45.0	51.9	62.5	80.9	45.5	52.9	63.6	77.0	43.9	52.0	61.4
	Bottom	61.2	39.1	39.1	46.6	61.4	39.7	39.8	47.1	57.3	39.1	39.2	45.4

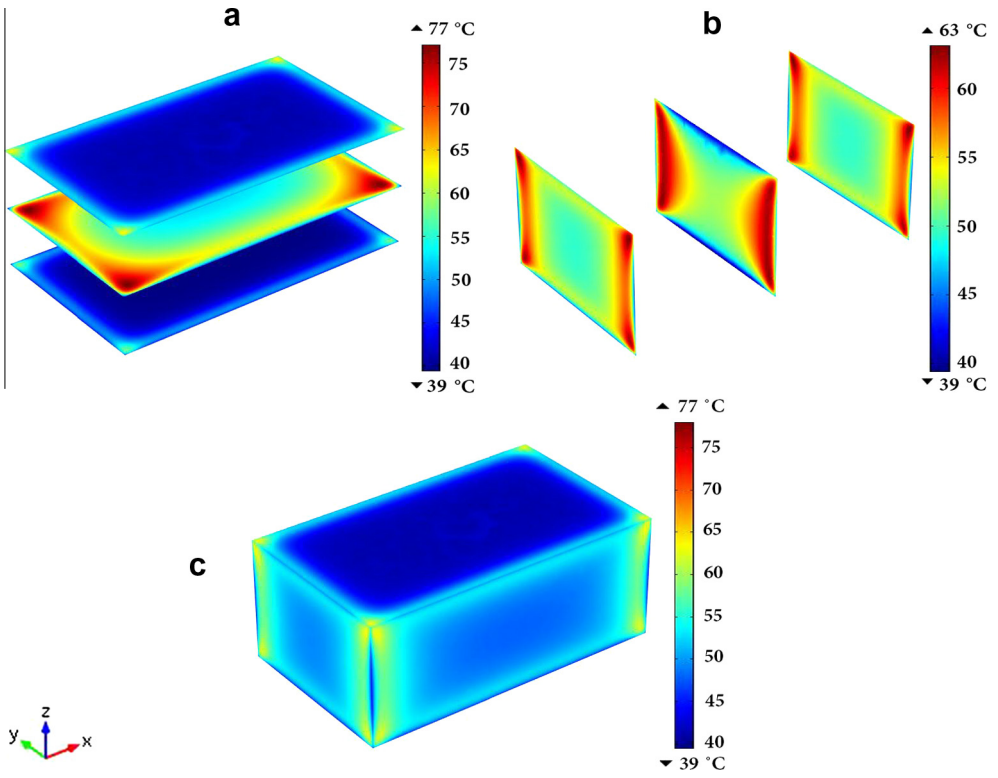

Fig. 7. Simulated (LLLE x Kopelman) temperature (°C) profiles of raisins sample (25.5 L × 15.0 W × 10.0 H cm^3) at (a) three horizontal layers (0, 5, and 10 cm), (b) three vertical layers (0, 12.8, and 25.5 cm), and (c) whole sample after 4 min RF heating with an electrode gap of 13.6 cm and initial temperature of 23 °C.

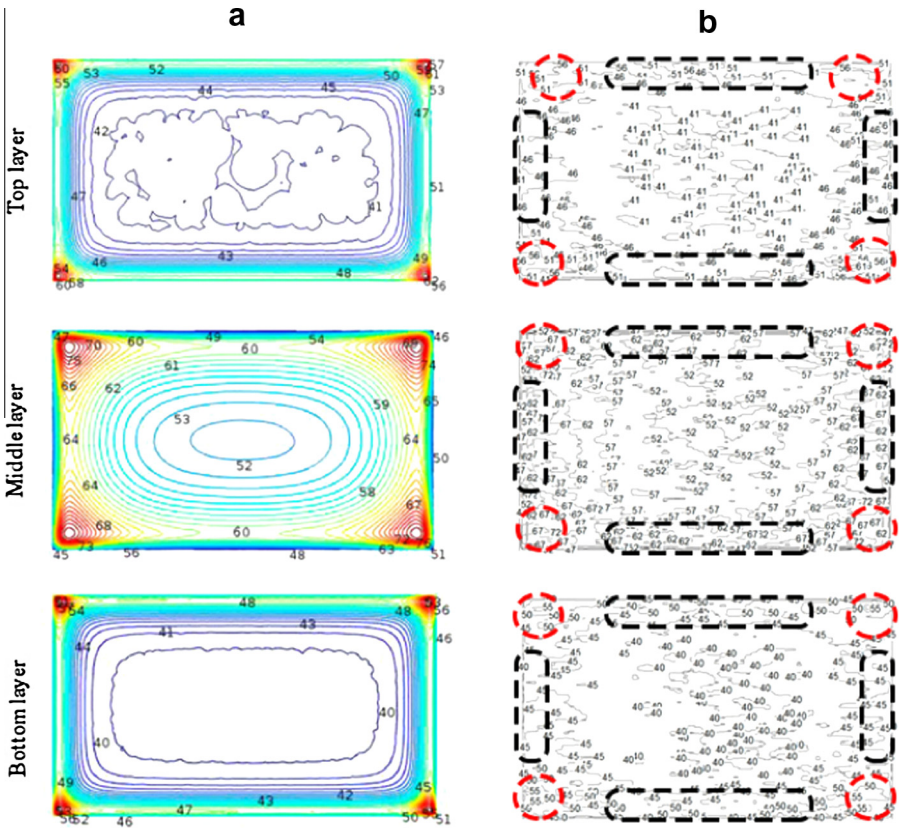

Fig. 8. Simulated (LLLE × Kopelman) (a) and experimental (b) temperature distributions of top, middle, and bottom layers of raisin samples placed in a polypropylene container (25.5 L × 15.0 W × 10.0 H cm^3) in the center and middle between the top and bottom electrodes of the RF system after 4 min heating at a fixed electrode gap of 13.6 cm and initial temperature 23 °C (Dash line areas have higher temperatures compared to other areas).

Table 6
Comparison between simulated (LLLE × Kopelman) and experimental average temperature ± standard deviation (°C) at three horizontal layers of raisin samples after 4 min RF heating at a fixed electrode gap of 13.6 cm and initial temperature of 23 °C.

Layer	Simulation (°C)	Experiment (°C)
Top	50.1 ± 4.50	45.7 ± 4.78
Middle	61.5 ± 6.62	57.2 ± 5.18
Bottom	45.8 ± 4.22	42.1 ± 3.40

Table 7
Relative sensitivity of UI of treated raisins samples with respect to ± 20% change of model input parameters.

Model parameters	Nominal value	Change in UI (%)
DPs (ε'–$j\varepsilon''$)	$(0.08 * T + 6.3) - j * (0.02 * T + 1.9)$	6.30
Electrical voltage, (V, V)	4100	3.70
Thermal conductivity, (k, W m^{-1} K^{-1})	$0.001 * T + 0.15$	2.28
Heat transfer coefficient, (h, W m^{-2} K^{-1})	20	0.65
Density, (ρ, kg m^{-3})	784	0.19
Specific heat, (Cp, J kg^{-1} K^{-1})	$10.9 * T + 1831$	0.09

*T is temperature in °C.

experimental and the simulation results in the central parts of the top, middle, and bottom layers comparable results were obtained. However, in corners and edges of the top, middle, and bottom layers, the maximum temperature differences were about 5, 7, and 3 °C, respectively, when comparing between the simulated and experimental data. Table 6 shows a comparison between the simulated and experimental average and standard deviation of temperature (°C) of raisins sample in three horizontal layers after 4 min RF heating at a fixed electrode gap of 13.6 cm and initial temperature 23 °C. About 4 °C difference was obtained between simulated and experimental average in all layers.

The UI was most sensitive to the dielectric properties of the heated samples, the electrical voltage of the top electrodes, and the thermal conductivity of the treated raisins, respectively; while the heat transfer coefficient, the density, and the specific heat of the samples have less effect on the UI. When changing the dielectric properties of the raisin samples by 20%, the UI changed 6.30%, whereas changing the heat transfer coefficient of the material by 20%, the UI changed 0.09% (Table 7).

4. Conclusions

A computer model of the RF heating for raisins was developed for a 6 kW, 27.12 MHz RF system using the finite element-based commercial software, COMSOL. The computer model was validated using experimental results. Good agreement was obtained when comparing the simulated and experimental temperatures in three horizontal layers of raisins packed in a rectangular container except for some corners with maximum difference of 7 °C. The simulated and the experimental results showed higher temperature values in the middle layers compared with those of the top and the bottom layers. Corners and edges were heated more than center areas in all layers. The model can be used to modify the top and bottom electrodes of the RF system to accommodate changes in sample shape and dimension to reduce the concentration of the electrical field at the corners and the edges of samples, thereby improving the heating uniformity of dried fruits exposed to RF treatment.

Acknowledgements

The authors acknowledge the financial support from King Saud University, Riyadh, Saudi Arabia for B. Alfaifi to pursue his Ph.D. degree at Washington State University (WSU) and funding from the Agricultural Research Center at WSU.

References

Alfaifi, B., Wang, S., Tang, J., Rasco, B., Sablani, S., Jiao, Y., 2013. Radio frequency disinfestation treatments for dried fruits: Dielectric properties. LWT – Food Science and Technology 50 (2), 746–754.
Barber, H., 1983. Electroheat, first ed. Granada Publishing Limited, London, UK.
Barreveld, W.H., 1993. Date palm products. FAO Agricultural Services Bulletin No. 101. Rome, Italy, FAO.
Birla, S.L., Wang, S., Tang, J., 2008. Computer simulation of radio frequency heating of model fruit immersed in water. Journal of Food Engineering 84 (2), 270–280.
Bottcher, C.J.F., 1945. The dielectric constant of crystalline powders. Recueil des Travaux Chimiques des Pays-Bas 64 (2), 47–51.
Chan, T.V., Tang, J., Younce, F., 2004. 3-Dimensional numerical modeling of an industrial radio frequency heating system using finite elements. Journal of Microwave Power and Electromagnetic Energy 39 (2), 87–105.
Choi, C.T.M., Konrad, A., 1991. Finite-element modeling of the RF heating process. IEEE Transactions on Magnetics 27 (5), 4227–4230.
COMSOL material library, COMSOL Multiphysics, V4.2a, 2012. Burlington, MA, USA.
Eucken, A., 1940. Allgemeine gesetzmassig keiten für das wärmeleitvermogen veschiedener stoffarten und aggregatzustande. Forschung Gebeite Ingenieur 11 (1), 6–20.
Fu, Y.C., 2004. Fundamentals and industrial applications of microwave and radio frequency in food processing. In: Smith, J.S., Hui, Y.H. (Eds.), Food Processing: Principles and Applications. Blackwell, Iowa, USA, pp. 79–100.
Johnson, J.A., Yahia, E.M., Brandl, D.G., 2009. Dried fruits and tree nuts. In: Yahia, E.M. (Ed.), Modified and Controlled Atmospheres for the Storage, Transportation, and Packaging of Horticultural Commodities. CRC Press, Taylor & Francis, Boca Raton, FL, pp. 507–526.
Kim, Y.R., Morgan, M.T., Okos, M.R., Stroshine, R.L., 1998. Measurement and prediction of dielectric properties of biscuit dough at 27 MHz. Journal of Microwave Power and Electromagnetic Energy 33 (3), 184–194.
Kopelman, I.J. (1966). Transient heat transfer and thermal properties in food systems. PhD dissertation, Michigan State University, East Lansing, MI.
Kraszewski, A., 1977. Prediction of the dielectric properties of two phase mixtures. Journal of Microwave Power and Electromagnetic Energy 12 (3), 215–222.
Landau, L.D., Lifshitz, E.M., 1960. Electrodynamics of Continuous Media. Pergamon Press, Oxford, England.
Liu, Y., Tang, J., Mao, Z., 2009. Analysis of bread loss factor using modified Debye equations. Journal of Food Engineering 93 (4), 453–459.
Looyenga, H., 1965. Dielectric constants of heterogeneous mixtures. Physica 31 (3), 401–406.
Marra, F., Lyng, J., Romano, V., McKenna, B., 2007. Radiofrequency heating of foodstuff: solution and validation of a mathematical model. Journal of Food Engineering 79 (3), 998–1006.
Marshall, M.G., Metaxas, A.C., 1998. Modeling of the radio frequency electric field strength developed during the RF assisted heat pump drying of particulates. Journal of Microwave Power and Electromagnetic Energy 33 (3), 167–177.
Metaxas, A.C., 1996. Foundations of Electroheat–A Unified Approach. John Wiley & Sons, New York.
Nelson, S.O., 1991. Dielectric properties of agricultural product measurements and applications. IEEE Transactions 26 (5), 845–869.
Nelson, S.O., 1992. Measurement and applications of dielectric properties of agricultural products. IEEE Transactions on Instrumentation and Measurement 41, 116–122.
Neophytou, R.I., Metaxas, A.C., 1996. Computer simulation of a radio frequency industrial system. Journal of Microwave Power and Electromagnetic Energy 31 (4), 251–259.
Neophytou, R.I., Metaxas, A.C., 1997. Characterisation of radio frequency heating systems in industry using a network analyser. IEE Proceedings-Science Measurement and Technology 144 (5), 215–222.
Neophytou, R.I., Metaxas, A.C., 1998. Combined 3D FE and circuit modeling of radio frequency heating systems. Journal of Microwave Power and Electromagnetic Energy 33 (4), 243–262.
Neophytou, R.I., Metaxas, A.C., 1999. Combined tank and applicator design of radio frequency heating systems. IEE Proceedings–Microwaves Antennas and Propagation 146 (5), 311–318.
Pimentel, D., Raman, K.V., 2002. Postharvest food losses to pests in India. In: Lal, Rattan, Hansen, David O., Uphoff, Norman, Slack, Steven A. (Eds.), Food Security and Environmental Quality in the Developing World. Blackwell, Iowa, USA, pp. 79–100.

Tiwari, G., Wang, S., Tang, J., Birla, S.L., 2011a. Computer simulation model development and validation for radio frequency (RF) heating of dry food materials. Journal of Food Engineering 105 (1), 48–55.

Tiwari, G., Wang, S., Tang, J., Birla, S.L., 2011b. Analysis of radio frequency (RF) power distribution in dry food materials. Journal of Food Engineering 104 (4), 548–556.

von Hippel, A.R., 1995. Dielectric Materials and Applications. Arctech House, Boston, USA.

Wang, J., 2007. Study of Electromagnetic Field Uniformity in Radio Frequency Heating Applicator. Doctor of Philosophy Dissertation. Department of Biological Systems Engineering. Washington State University, Pullman, WS, USA.

Wang, S., Monzon, M., Johnson, J.A., Mitcham, E.J., Tang, J., 2007a. Industrial-scale radio frequency treatments for insect control in walnuts: I. Heating uniformity and energy efficiency. Postharvest Biology and Technology 45 (2), 240–246.

Wang, S., Monzon, M., Johnson, J.A., Mitcham, E.J., Tang, J., 2007b. Industrial-scale radio frequency treatments for insect control in walnuts: II. Insect mortality and product quality. Postharvest Biology and Technology 45 (2), 247–253.

Wang, S., Tang, J., Hansen, J.D., 2007c. Experimental and simulation methods of insect thermal death kinetics. In: Tang, J., Mitcham, E., Wang, S., Lurie, S. (Eds.), Heat Treatments for Postharvest Pest Control: Theory and Practice. CABI Publishing, Oxon, UK, pp. 105–132.

Wang, S., Tang, J., Johnson, J.A., Hansen, J.D., 2002. Thermal-death kinetics of fifth-instar *Amyelois transitella* (Walker) (Lepidoptera: Pyralidae). Journal of Stored Products Research 38 (5), 427–440.

Wang, S., Tiwari, G., Jiao, S., Johnson, J.A., Tang, J., 2010. Developing postharvest disinfestation treatments for legumes using radio frequency energy. Biosystems Engineering 105 (3), 341–349.

Wang, S., Yue, J., Tang, J., Chen, B., 2005. Mathematical modelling of heating uniformity of in-shell walnuts in radio frequency units with intermittent stirrings. Postharvest Biology and Technology 35 (1), 97–107.

Yang, J., Zhao, Y., Wells, J.H., 2003. Computer simulation of capacitive radio frequency (RF) dielectric heating on vegetable sprout seeds. Journal of Food Process Engineering 26 (3), 239–263.

Yang, S-I., Pearce, J.A., 1989. Boundary condition effects on microwave spatial power deposition patterns. Center for Energy Studies, Balcones Research Center, the University of Texas, Austin, TX, USA.